Microchim Acta (2017) 184:4637–4646
DOI 10.1007/s00604-017-2500-0

ORIGINAL PAPER

Voltammetric determination of nitrite by using a glassy carbon electrode modified with a self-assembled nanocomposite prepared from CdTe quantum dots, cetyltrimethylammonium bromide, chitosan and multiwalled carbon nanotubes

Jie Hu[1] · **Feng Guo**[2] · **Li Wang**[1]

Received: 26 May 2017 / Accepted: 2 September 2017 / Published online: 16 September 2017

Abstracts The authors describe an electrostatic self-assembly strategy for the modification of a glassy carbon electrode (GCE) with CdTe quantum dots (QDs), cetyltrimethylammonium bromide, chitosan, and multiwalled carbon nanotubes (MWCNTs). The nanocomposite was characterized by scanning electron microscopy revealing the distribution of spherically shaped CdTe QDs on the tubular networks of the MWCNTs. The modified GCE is shown to enable improved voltammetric sensing of nitrite, best at a working potential of 0.78 V (vs. SCE). The synergetic effect of the four components leads to rapid electron transfer and in an increased active area. Hence, excellent electrocatalytic activity towards the oxidation of nitrite is observed. Square wave voltammetry was applied to quantify nitrite, and the two linear ranges cover the 1 to 100 μmol L^{-1} and 100 to 600 μmol L^{-1} nitrite concentration ranges. The detection limit is 0.30 μmol L^{-1}. The method was applied to the determination of nitrite in pickled vegetables and the results were compared to a UV-Vis method. The method is found to be sensitive, accurate, rapid, and well repeatable.

Keywords SWV determination · Nitrite sensor · CdTe QD-CTAB/Chit-MWCNT nanocomposite · Modified glassy carbon electrode · Electrostatic self-assembly strategy · Pickled vegetables

Electronic supplementary material The online version of this article (https://doi.org/10.1007/s00604-017-2500-0) contains supplementary material, which is available to authorized users.

✉ Li Wang
liwang_wh@mail.zjgsu.edu.cn

[1] Department of Applied Chemistry, College of Food Science and Biotechnology, Zhejiang Gongshang University, No.18, Xuezheng St., Xiasha University Town, Hangzhou 310018, China

[2] Narada Power Source Co., Ltd., Hangzhou 310012, China

Introduction

During their lactic acid fermentation bioprocessing procedure when pickled vegetables are made, nitrite is produced through reduction reaction of nitrate naturally presented in fresh raw vegetable tissues catalyzed by reductase [1]. The nitrite ions can interact with amines to form N-nitrosamines, which might cause cancer and hypertension and be harmful to human health by long-term ingestion of foods containing nitrite [1, 2]. Therefore, the limitation of nitrite in food is restricted in a limited level. For example, the maximum limit of 20 mg Kg^{-1} has been set in pickled food in China; World Health Organization has fixed the maximum limit of 3 mg L^{-1} for nitrite in drinking water. Thus, a number of methods have been developed for nitrite determination.

For the analysis of nitrite, compared with the mainly used methods such as spectrometry [3] and ion chromatography [4], which suffered from some disadvantages of serious interferences, tedious sample pretreatment (e.g. derivatization), and time-consuming. As an alternative choice, electrochemical method measuring the current generated by direct nitrite oxidation at electrodes was proved to be high sensitivity, easy operation and the possibility for the construction of portable devices for fast screening purposes [5, 6]. However, due to the high over potential of nitrite at bare electrode, for example, glassy carbon electrode vs saturated calomel electrode (SCE) (0.89 V), the interference possibly caused by the co-existing components became a serious issue. To improve its selectivity and sensitivity, a couple of sensing chemicals including but not limited to metal [7–9], metal oxide nanoparticles [10, 11], metal oxide-metal [12], and polymers (polyvinylimidazole) [13] showed electrocatalytic activity for the oxidation of nitrite and reduced nitrite oxidation potential.

Quantum dot (QD), a novel semiconductor nanocrystal with average diameter of 2–20 nm, has been placed on

significant emphasis because of its high fluorescence efficiency and significantly quantum size effect. A highly sensitive and selective method for the determination of nitrite was established based on the electrochemiluminescent (ECL) of CdTe [14] or quenching of the ECL of CdSe QDs [15]. QDs also showed promising prospects as electrode modified materials in developing electrochemical sensors due to their very small size, high electron-transfer efficiency, and large specific surface area [16]. However, nitrite sensor based on QDs modified electrode hasn't been investigated possibly due to the challenge of the stability of the direct immobilization of QDs onto the surface of GCE. Fortunately, QDs can be covalently attached to amino functionalized molecules via the QDs capping, consisting of carboxylic acid functionalities such as thioglycollic acid (TGA) [17]. They also can attached to positively charged molecules via electrostatic self-assembly due to its negatively charged carboxylic acid functionalities [18, 19]. Based on its properties, in this study, the immobilization of QDs onto the GCE will carried out via electrostatic self-assembly strategy due to its simplicity.

Chitosan (Chit), a positively charged natural polysaccharide with primary amino groups in the polymer chain, shows excellent capability for film formation, nontoxicity, good adhesion, mechanical strength, and good water permeability. The hybrid systems of chitosan and multiwalled carbon nanotubes (MWCNTs) have received increasing attention due to their attractive structural, mechanical and electrical properties. They find wide applications in electrochemical sensor and biosensor fabrication [20, 21]. Cetyltrimethylammonium bromide (CTAB), a positive charged small molecular weight detergent with a long hydrophobic chain, is easily assembled with electronegative QDs, simultaneously, CTAB molecule can be hydrophobic adsorbed on the hydrophobic surface of carbon nanotubes (CNTs), improve the solubility of CNTs in water [22].

Herein, we report on the fabrication of an electrochemical sensor using glassy carbon electrode modified with CdTe QD-CTAB-Chit-MWCNT nanocomposite via electrostatic self-assembly strategy, the electrode coupled with square wave voltammetry (SWV) were finally applied in the determination of nitrite in the extraction of commercial pickled vegetable samples. As showed in Scheme 1, MWCNTs dispersed in chitosan form a stable film at the electrode, simultaneously, the negative charged TGA capped CdTe QDs attached to positively charged chitosan, and thus a nanostructured platform was created. Considering the stereospecific blockade effect possibly caused by chitosan due to its high molecular weight [23], CTAB was introduced into the nanocomposite via hydrophobic adsorption on the hydrophobic surface of MWCNTs, thus more CdTe QDs were attached to the electrode via electrostatic absorption to CTAB, forming a compact structure and stable nanocomposite, the electron transport activity of the nanocomposite film for nitrite analysis might be improved. In fact, CdTe QD-CTAB/Chit-MWCNT nanocomposite was proved to be more stable than any other combination of the four components. Moreover, the highest current peak at the relatively lowest potential of nitrite was obtained on the electrode. To our knowledge, an electrode based on CdTe QD-CTAB/Chit-MWCNT nanocomposite modified glassy carbon electrode via electrostatic self-assembly strategy for the sensing of nitrite has not been reported.

Experimental

Materials and reagents

MWCNTs were obtained from Shenzhen SUSN SINOTECH New Materials Co., Ltd. (http://www.susnzk.cn). Chitosan was

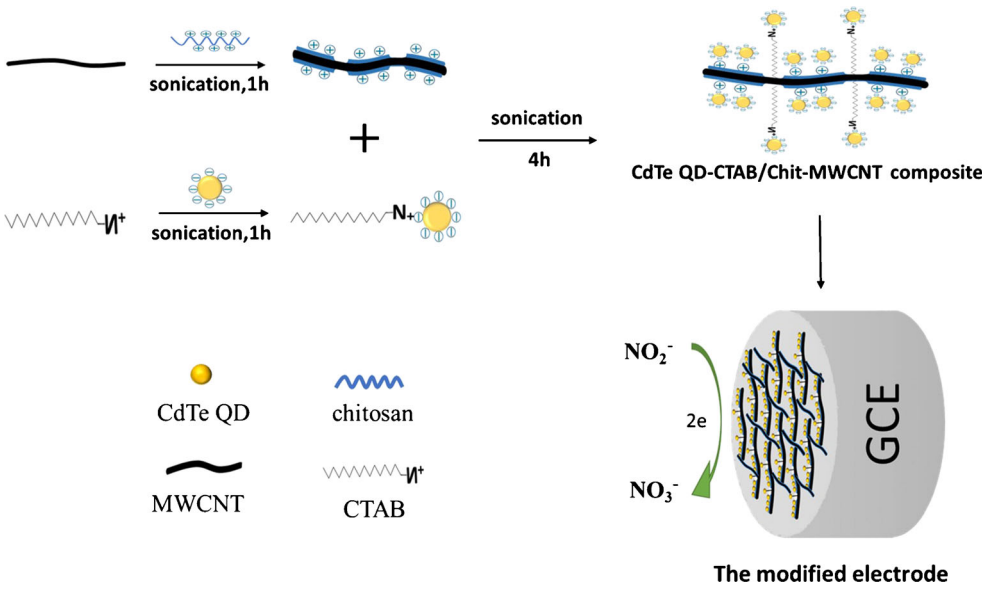

Scheme 1 Schematic illustration of the procedure of the modification of a glassy carbon electrode (GCE) with CdTe quantum dots (QDs), cetyltrimethylammonium bromide (CTAB); chitosan (Chit) and multiwalled carbon nanotubes (MWCNTs)

purchased from Sigma-Aldrich, China (http://www.sigmaaldrich.com/china-mainland.html). All other chemicals were purchased from Aladdin (Shanghai, China, http://www.aladdin-e.com). All chemicals and reagents were of analytical grade without further purification. Ultra-pure water was prepared by a Milli-Q purification system (Millipore, USA, http://millipore.bioon.com). All electrochemical tests were carried out in phosphate buffer (0.1 M Na_2HPO_4-NaH_2PO_4, pH 4.0 and adjusting the pH with H_3PO_4 or NaOH).

Apparatus

Cyclic voltammetry (CV) and Square wave voltammetry (SWV) used in all electrochemical experiments were carried out on an LK2005A electrochemical workstation (Lanlike, China, http://www.lanlike.com), in connection with a personal computer. A modified glassy carbon used as the working electrode for electrochemical experiments, a platinum foil as auxiliary, and the SCE was used as the reference electrode. The pH value was measured with a Sartorius pH meter, model PB-10 (http://www.sartorius-weighing.com.cn). Electrochemical impedance spectroscopy (EIS) was performed using a ParStat4000 electrochemical workstation (http://www.ametek.com). Characterization of morphology and microstructure was performed by scanning electron microscope (SEM) JEOL JSM-6510 (Japan, https://www.jeol.co.jp/en).

Preparation of CdTe QD-CTAB/Chit-MWCNT nanocomposite

CdTe QD were synthesized using a modified method according to the procedure described in the literature [24]. Briefly, 253.4 mg tellurium powder and 225 mg sodium borohydride in 10 mL ultrapure water were added to the 50 mL three-necked flask under stirring and high purity nitrogen purging. The flask was heating in a water-bath at 40 °C until the tellurium powder completely dissolved and the color of solution was changed from violet to white. The fresh NaHTe precursor solution was obtained. Then, the fresh NaHTe solution was added to 200 mL $CdCl_2$ solution (4 mmol L^{-1}) containing 750 μL TGA in a 250 mL three-necked flask and the pH of the mixed solution was adjusted to 11.0 by 1 mol L^{-1} NaOH using pH meter under N_2 atmosphere. The final molar ratio of Te^{2-}:Cd^{2+}: TGA was fixed at 1:2:5. Then the solution was heated and refluxed at 95 °C for 4 h to obtain the CdTe QDs.

0.5% chitosan suspension was prepared by adding the chitosan powder into 1% acetic acid and 0.5% CTAB suspension was prepared by adding CTAB into ultrapure water, respectively. An aqueous solution of the synthesized CdTe QDs was added to 1.0 mL of 0.5% CTAB suspension, and then sonicated for 1 h to prepare CTAB-CdTe QD composite. MCNTs-Chit composite was prepared by adding 7.5 mg MWCNTs to the mixed solution of 0.5 mL 0.5% chitosan suspension and 0.5 mL of DMF with the aid of ultrasonication for 1 h. CdTe-CTAB/Chit-MWCNT nanocomposite was finally prepared by transferring 0.25 mL CTAB-CdTe QD into 0.5 mL of MWCNT-Chit composite with the aid of ultra-sonication for 4 h.

Fabrication of the electrochemical sensor

For fabricating CdTe QD-CTAB/Chit-MWCNT/GCE, the bare GCE was polished to a mirror-like surface with 0.03 mm α-alumina slurry and rinsed thoroughly with ultrapure water, and then sonicated in ultrapure water and ethanol for 5 min, respectively. 5.0 μL of the CdTe QD-CTAB/Chit-MWCNT nanocomposite was deposited on the polished GCE surface. After drying under an infrared lamp, the as denoted CdTe QD-CTAB/Chit-MWCNT/GCE was fabricated. The MWCNT/GCE, MWCNT-Chit/GCE, CTAB-MWCNT-Chit/GCE, MWCNT-Chit-CdTe QD/GCE and CTAB-CdTe QD-Chit/GCE were similarly prepared.

Electrochemical measurements

Under optimum conditions, all electrochemical experiments were carried out in the electrochemical cell at room temperature (25 ± 2 °C). 10 mL of phosphate buffer (0.1 M, pH = 4.0) containing a different concentration of sodium nitrite standard solution or the extraction of pickled vegetable sample was added into the cell and the three-electrode system installed. Before each electrochemical experiment, the prepared modified electrode was immersed in phosphate buffer (0.1 M, pH = 4.0) and then cyclic voltammetry (CV) was conducted from 0 to 0.8 V with the scan rate of 50 mV s^{-1} until the detection signal stabilized after scanning about 14 cycles. Square wave voltammetry (SWV) experiments were conducted using the increment potential of 0.004 V, frequency of 15, and amplitude of 0.024 V over the potential range of 0.4–1.0 V versus SCE.

Analysis of the pickled vegetable samples

The pickled vegetable samples were obtained from local market (Hangzhou, China). 5 g of each sample was crushed and mixed with 12.5 mL saturated borax solution. 5 ml of 30% zinc acetate was added to the mixture in order to precipitate protein and the mixture was then heated at 70 °C for 15 min in a water bath. After being cooled to room temperature, the upper oil layer was removed and then the mixture was filtered and diluted to 50 mL [12]. The resulting sample solution was stored at 4 °C for the next test.

Results and discussion

Characterization of CdTe QD-CTAB/Chit-MWCNT composite

The morphology and microstructure of the MWCNTs (A), MWCNT-Chit (B), CdTe QDs (C) and CdTe QD-CTAB/Chit-MWCNT (D) nanocomposite coated on the surface of the electrodes were characterized by SEM (Fig. 1). Figure 1a and b show the tubular networks of MWCNTs and the MWCNT-Chit composite, respectively. From Fig. 1c, it can be seen that CdTe nanoparticles were of relatively uniform spherical shape. The SEM micrograph of CdTe QD-CTAB/Chit-MWCNT nanocomposite (Fig.1d) shows the tubular networks of MWCNTs with distribution of globular structure, which may indicate the decoration of CdTe QDs to the surface of MWCNTs.

EIS and CV studies on CdTe QD-CTAB/Chit-MWCNT modified electrode

Electrochemical impedance spectroscopy (EIS) is an efficient tool for studying the impedance changes of surface-modified electrode during the fabrication process. The electron-transfer resistance at the electrode surface is equal to the semicircle diameter of the Nyquist plots and can be used to describe the interface properties of the modified electrode [25]. As seen in Fig. 2a, the Nyquist plot of MWCNT-Chit/GCE (b) is almost linear suggesting the good electron transfer capability of MWCNT-Chit composite film [18]. Compared to bare GCE (a), the impedance obviously increased upon addition of CdTe QD-CTAB composite on the surface of GCE (c). The possible reason is that CdTe QDs are semiconductors and its conductivity is not as good as MWCNT-Chit composite [26]. However, the semicircle portion at higher frequencies became extremely small after addition of CdTe QD-CTAB composite to the MWCNT-Chit composite (d), indicating that CdTe QD-CTAB composite was successful modified on the surface of MWCNT-Chit composite. Fig. 2b is the cyclic voltammogram (CV) curves of the modified electrodes recorded in the presence of 1 mM $[Fe(CN)_6]^{3-/4-}$ in 0.1 M KCl solutions. The redox peak currents of $[Fe(CN)_6]^{3-/4-}$ at the surface of bare GCE (a), MWCNT-Chit/GCE (b), CdTe QD-CTAB/GCE (c) and CdTe QD-CTAB/Chit-MWCNT/GCE (d) fitted well with the results of prior studies of EIS at the modified electrodes.

Electrochemical behavior of nitrite on modified electrode

As shown in Fig. 3, cyclic voltammetry was conducted to study the electrochemical behavior of 0.1 mM nitrite in phosphate buffer (0.1 M, pH = 4.0) at the bare GCE (a), MWCNT/GCE (b), MWCNT-Chit/GCE (c), CTAB-

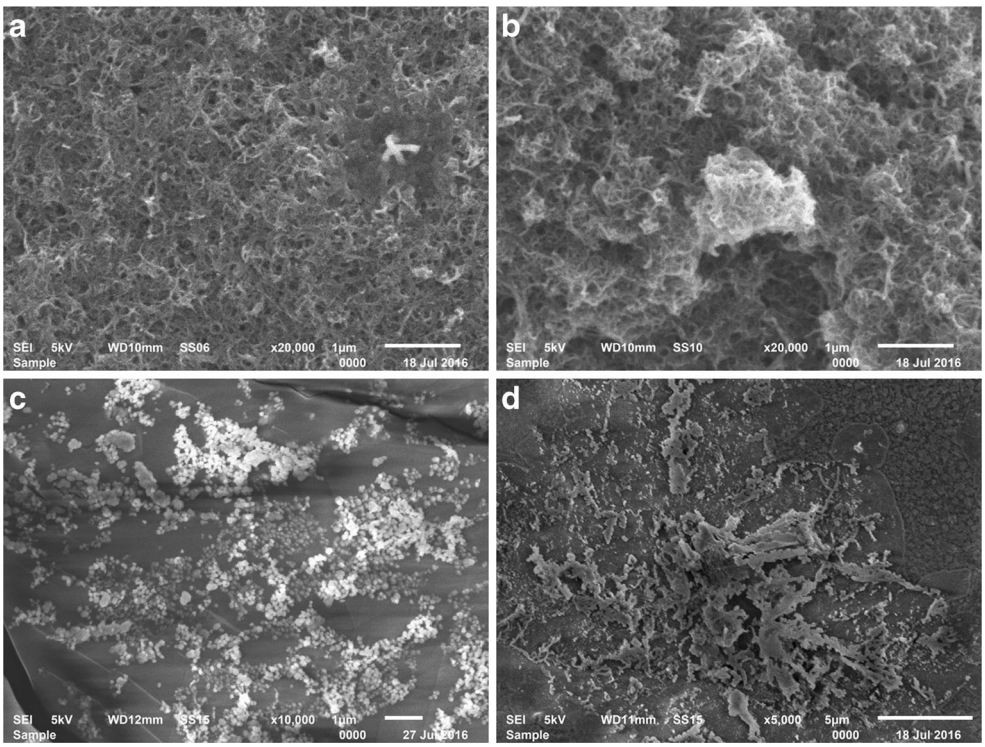

Fig. 1 SEM micrographs of (**a**) MWCNTs, (**b**) MWCNT-Chit, (**c**) CdTe QDs and (**d**) CdTe QD-CTAB/Chit-MWCNT

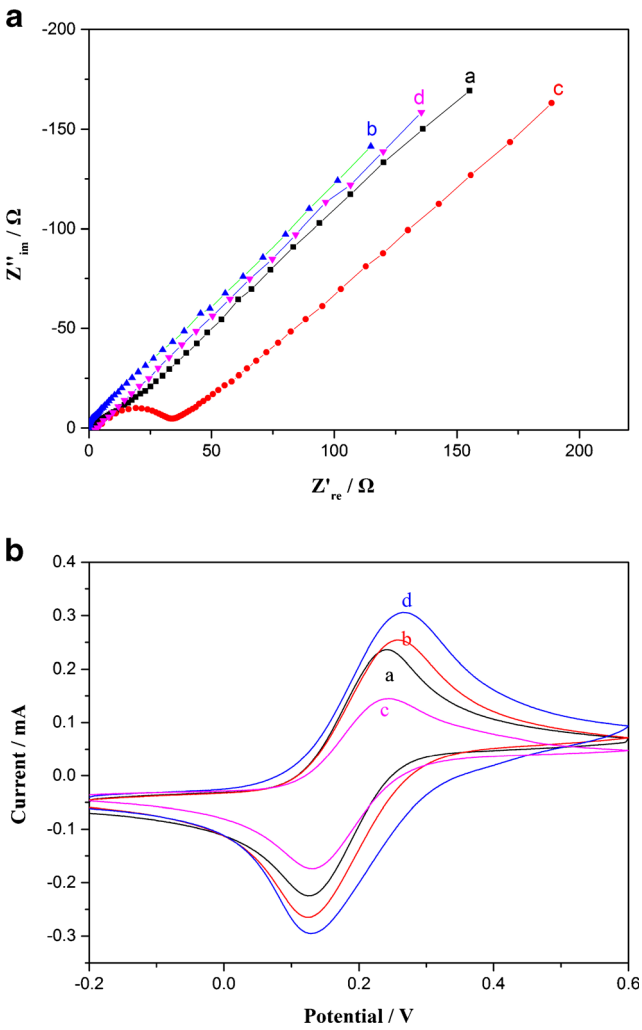

Fig. 2 **a** The Nyquist plots and (**b**) CV behavior of the modified GCE in 1 mM $[Fe(CN)_6]^{3-/4-}$ solution containing 0.1 M KCl. Scan rate: 50 mV s^{-1}. a: bare GCE, b: MWCNT-Chit/GCE, c: CdTe QD-CTAB/GCE and d: CdTe QD-CTAB/Chit-MWCNT/GCE. Reference electrode: SCE

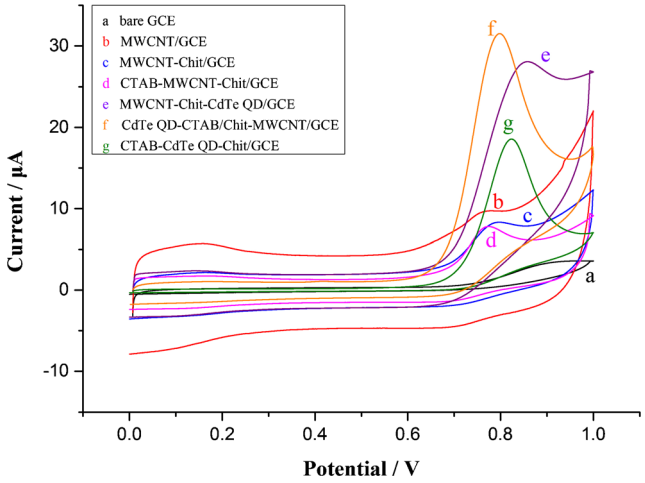

Fig. 3 Cyclic voltammetric behavior of 0.1 mM nitrite in 0.1 M phosphate buffer (pH = 4.0) at bare GCE (a), MWCNT/GCE b), MWCNT-Chit/GCE (c), CTAB-MWCNT-Chit/GCE (d), MWCNT-Chit-CdTe QD/GCE (e), CdTe QD-CTAB/Chit-MWCNT/GCE (f) and CTAB-CdTe QD-Chit/GCE (g). Scan rate: 50 mV s^{-1}. Reference electrode: SCE

MWCNT-Chit/GCE (d), MWCNT-Chit-CdTe QD/GCE (e), CdTe QD-CTAB/Chit-MWCNT/GCE (f), and CTAB-CdTe QD-Chit/GCE (g). As seen, the nitrite oxidation peak at bare GCE was rather weak and the oxidation potential was observed at around 0.895 V (a). Compared to the bare GCE, the oxidation potential of nitrite at MWCNT/GCE negatively shifted to 0.760 V with an approximately equal oxidation current and much higher background currents (b). When Chit was added to MWCNTs to fabricate a stable MWCNT-Chit mixture, the background current of nitrite at MWCNT-Chit/GCE (c) obviously decreased about a half than that at MWCNT/GCE (b). Taking the efficient advantages of the stable hybrid system of MWCNT-Chit, CdTe QDs was electrostatic decorated to the surface of MWCNT-Chit, a dramatically enhanced peak (e) was observed, suggesting the well performed electrocatalytic behavior of CdTe QDs. To further improve the selectivity and sensitivity of the MWCNT-Chit-CdTe QD modified electrode, CTAB, a positively charged small molecular surfactant, was introduced in the nanocomposite to compensate the stereospecific blockade effect possibly caused by Chit due to its polymer chain to enable more CdTe QDs attached to the modified GCE, it was observed that at CdTe QD-CTAB/Chit-MWCNT/GCE, a narrow and well-shaped as well as enhanced oxidation peak of nitrite at a relatively low potential of 0.780 V was obtained (f) compared with curve e. Whereas, with the absence of CdTe QDs, when CTAB combined with MWCNT-Chit was used, the oxidation peak current (d) of nitrite was approximately the same as that at MWCNT-Chit (c), indicating CdTe QDs played an important electrocatalytic role at the CdTe QD-CTAB/Chit-MWCNT/GCE. With the absence of CTAB, when CdTe QDs combined with MWCNT-Chit was used, the oxidation peak was at a relative high potential (e) with lower current, indicating that the introduction of CTAB probably enabled more CdTe QDs modified in the surface of MWCNT-Chit composite film, which worked as an electrocatalyst, simultaneously, CTAB was contribute to the relatively lower nitrite oxidation potential. Moreover, with the absence of MWCNT when CTAB-CdTe QD-Chit/GCE (g) was used, compared with CdTe-CTAB/Chit-MWCNT/GCE, a relatively lower peak current at higher potential was obtained, indicating MWCNT contributed positively to the peak signal of nitrite as well. Overall, the enhanced peak current and negatively shifted potential was contributed to the synergy effect of the four components of MWCNTs, Chit, CdTe QDs and CTAB, leading

to the excellent electron transfer capability and increased active area at the surface of the modified electrode.

Furthermore, linear sweep voltammetry (LSV) was carried out to investigate the effect of scan rate on the electrochemical behavior of 0.05 mM nitrite at the CdTe QD-CTAB/Chit-MWCNT/GCE. As shown in Fig. 4, the oxidation peak currents (I_p) of nitrite increased gradually with the increase of the square root of scan rate ($v^{1/2}$) from 0.01 to 0.1 V s^{-1} in phosphate buffer (pH = 4.0). The linear relationship was obtained by plotting the I_p against $v^{1/2}$, indicating that the oxidation of nitrite on the modified electrode was a diffusion controlled process. The linear regression can be expressed as Ip = 96.489 $v^{1/2}$ - 2.790 (R^2 = 0.9947) (inset of Fig. 4). The peak potential E_p can be represented by the following formula for irreversible reaction process:

$$E_p = A + 2.3RT[2(1-\alpha)n_\alpha F]^{-1} log v \quad (1)$$

Where α is transfer coefficient, n_α is the number of electrons in the rate-limiting step, v is the scan rate and the remaining symbols have their usual meaning. A good linear relationship with E_p and log$v$ can be seen and the linear regression can be expressed as E_p = 0.086log$v$ + 0.941, R^2 = 0.9959. (Fig. S1). According to the Eq. (1), (1 - $\alpha)n_\alpha$ was calculated to be 0.34 and the Tafel slope (b = 2.3RT[(1 - $\alpha)n_\alpha F]^{-1}$) was then obtained to be 170 mV/dec, which is much higher than the normal values of 30–120 mV/dec, indicating that the rate-limiting step is the first one-electron transfer for the electrocatalytic oxidation of nitrite [27]. For the numbers of electrons n in the overall reaction can be calculated from the slop of I_p against $v^{1/2}$ according to the Eq. (2) which is applied to a totally irreversible process controlled by diffusion [28]:

$$I_p = 2.99 \times 10^5 n[(1-\alpha)n_\alpha]^{1/2} C_o A D^{1/2} v^{1/2} \quad (2)$$

Where C_o is the concentration of the nitrite, A is the electrode area, D is diffusion coefficient (for nitrite, 3.7 × 10^{-5} cm^2/s [29]) and the remaining symbols have been described above. Then the value of n was calculated to be 1.93, suggesting that the overall oxidation of nitrite proceeds by electron transfer followed by homogeneous disproportionation of NO_2 to nitrate and nitrite (Eqs. 3 and 4) [30]:

$$NO_2^- \rightarrow NO_2 + e^- \quad (3)$$

$$2NO_2 + H_2O \rightarrow NO_2^- + NO_3^- + 2H^+ \quad (4)$$

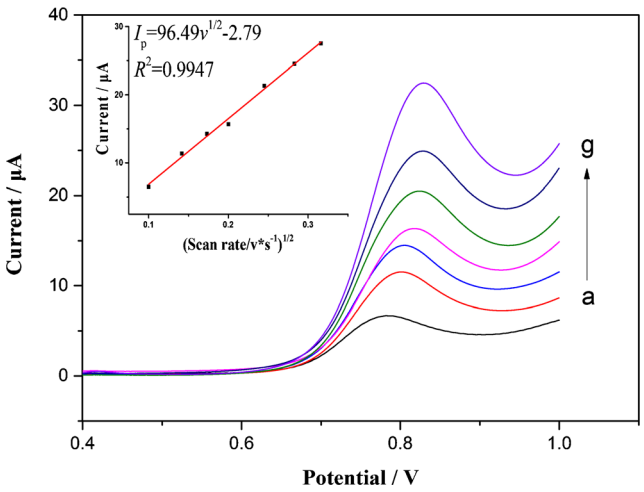

Fig. 4 LSVs obtained for nitrite (0.05 mM) at the CdTe QD-CTAB/Chit-MWCNT/GCE vs SCE at different scan rates (0.01, 0.02, 0.03, 0.04, 0.06, 0.08 and 0.1 V s^{-1}), inset shows plot of Ip versus $v^{1/2}$ in phosphate buffer (0.1 M, pH = 4.0)

Effective electrode area determined by Chronocoulometry

Figure S2a shows the chronocoulometry of MWCNT-Chit/GCE (b) and CdTe QD-CTAB/Chit-MWCNT/GCE (a) in 0.1 mol L^{-1} KCl containing 1.0 mmol L^{-1} $[Fe(CN)_6]^{3-}$, and Fig. S2b shows the relationship between the charge (Q) and the square root of time ($t^{1/2}$). As seen, the plot of Q of $[Fe(CN)_6]^{3-}$ changes linearly with $t^{1/2}$ at both MWCNT-Chit/GCE (b) and CdTe QD-CTAB/Chit-MWCNT/GCE (a), which can be expressed as Q_a = 2.82 × 10^{-4} $t^{1/2}$ + 4.56 × 10^{-4} and Q_b = 1.99 × 10^{-4} $t^{1/2}$ + 4.28 × 10^{-5}, respectively. According to the formula:

$$Q = \frac{2nFAcD^{1/2}t^{1/2}}{\pi^{1/2}} + Q_{dl} + Q_{ad} \quad (5)$$

Where c is the bulk concentration of $[Fe(CN)_6]^{3-}$, Q_{dl} is the coulombs required for double layer charging, Q_{ad} is the Faradaic charge, D is the diffusion coefficient of $[Fe(CN)_6]^{3-}$, which is a constant of 7.6 × 10^{-6} cm^2 s^{-1} in the given 1.0 mmol L^{-1} $[Fe(CN)_6]^{3-}$ in 0.1 mol L^{-1} KCl solution. A is the surface area of working electrode, and other symbols have their usual meanings. Here n = 1, the electron transfer number in overall reaction, Comparing of the slopes of the two electrodes with Eq. (5), the effective area of A_a and A_b were calculated to be 0.94 cm^2 and 0.66 cm^2, respectively, revealing that the effective area of CdTe QD-CTAB/Chit-MWCNT modified electrode is about 1.5 times as large as that of MWCNT-Chit electrode, which indicating the synergistic effect of CdTe QDs and CTAB are of importance role to enhance the capability of electrocatalytic oxidation of NO_2^-at CdTe QD-CTAB/Chit-MWCNT/GCE.

Analytical figures of merit

Experimental parameters such as the ratio of CTAB to CdTe QDs, the pH was optimized (Fig. S3). Under optimized experiment conditions, SWV was employed to acquire the analytical curve for nitrite. SWVs obtained after successive additions of the nitrite standard solution at CdTe QD-CTAB/Chit-MWCNT/GCE are shown in Fig. 5a and the analytical curves are in Fig. 5b. As seen, there are two good linear relationships with the nitrite concentration in the range from 1 to 100 μM and 100 to 600 μM, respectively. The linear regression can be expressed as I_{pa} (μA) = 0.15c (μM) - 0.30, R^2 = 0.9985; I_{pb} (μA) = 0.043c (μM) + 11.28, R^2 = 0.9917. It is noticed that in the low concentration range of nitrite, the slope of calibration curve is relatively larger compared with that in high concentration range. The possible reason is that when the nitrite concentration was low,

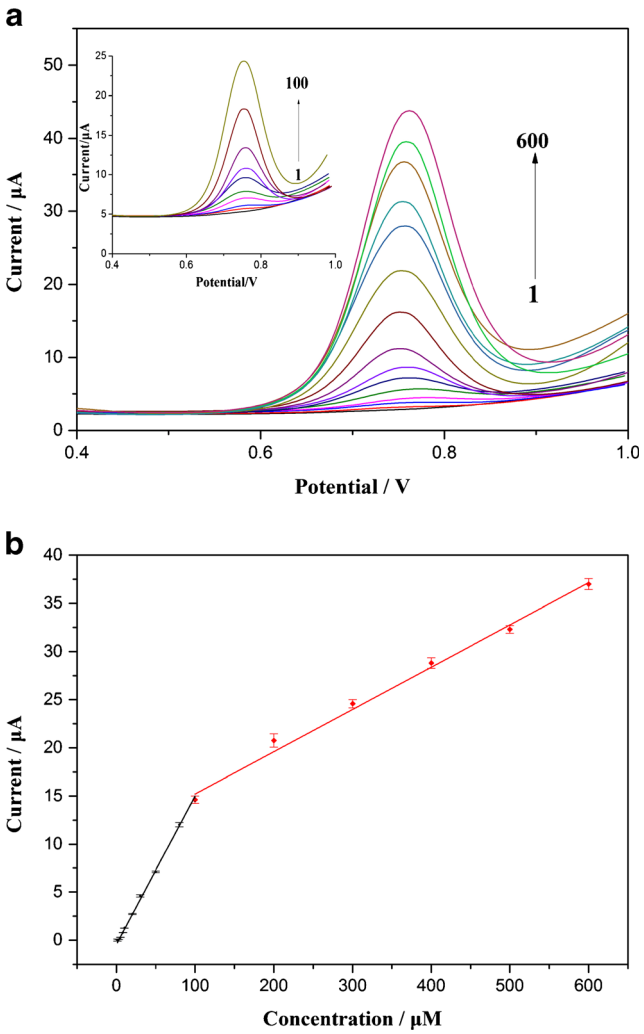

Fig. 5 **a** Square wave voltammograms of nitrite concentration ranged from 1 to 600 μmol L^{-1} in phosphate buffer (pH 4.0) at CdTe QD-CTAB/Chit-MWCNT/GCE vs SCE, and (**b**) the corresponding linear relationship between magnitude of anodic currents and nitrite concentrations from 1 to 100 μmol L^{-1} and 100–600 μmol L^{-1}. Inset of Fig.5a is square wave voltammograms of nitrite concentration ranged from 1 to 100 μmol L^{-1}

NO_2^-near the surface of modified electrode can be rapidly depleted as the substrates converted into products by the catalysis of CdTe QDs, resulting in a high sensitivity of the modified electrode. Whereas, when the nitrite concentration was high, the converting from NO_2^- to NO_3^-underwent a relatively long period of time, as well as the possibility of fouling effect at the modified electrode, thus resulting in a lower slope.

Additionally, the limit of detection (LOD) of 0.30 μM was obtained by calculating based on the equation of $DL = 3 \times SD$ (standard deviation) / slope. By comparison with the reported modified electrodes for the determination of nitrite listed in Table 1, the modified electrode in our work performs well in terms of high sensitivity and selectivity, as well as wide linear range.

The fabrication repeatability of the modified electrode was estimated by the measurements of 0.05 mM nitrite solution in phosphate buffer using five CdTe QD-CTAB/Chit-MWCNT/GCE made in three successive days and the relative standard deviation (RSD) of 3.13% was obtained. After 1 week when kept at 4 °C, the response signal at the modified electrode remained more than 95.5% of its original values. The above experiments results revealed good repeatability and stability of CdTe QD-CTAB/Chit-MWCNT modified electrode for the determination of nitrite.

To evaluate the recovery of the method, the extract solution of pickled samples spiked with nitrite at the levels of 20.0 mg Kg^{-1} was detected. The results showed that the recovery was between 98.2% and 101.1%, with a RSD ranged between 2.7% and 4.4%.

Interferences

The suitability of the electrochemical sensor mainly depends on the influence of interfering species presented in real samples along with nitrite. The interference influence on the sensor has been investigated in 0.1 mM nitrite solution with addition of cations, anions and organics. There are almost no interference on the detection of NO_2^-(0.1 mM) in the presence of 100 fold concentration of Na^+, K^+, Zn^{2+},Cd^{2+}, Cu^{2+}, Cl^-, SO_4^{2-}, CO_3^{2-}, as well as 10 fold NO_3^-, glucose and d-fructose which is due to the response signal change being less than ±5%. When 10 fold SO_3^{2-} was added into 0.1 mM nitrite solution, the response signal decreased more than 50%. In order to eliminate the interference of SO_3^{2-}, 72 μM methanal was included in the nitrite solution and then the oxidation peak current of NO_2^- recovered to original value. This probably happened because of the reaction of formaldehyde with sodium sulfite to form formaldehyde bisulfite

Table 1 Comparison of the performances of some different NO_2^- sensors employed carbon materials and metal nanoparticles as the substrates

Method	Modified electrode	E_p (V)	Linear range (μmol l^{-1})	LODs (μmol l^{-1})	Sample matrix	Ref
DPV	PATP[a]-Pt_{nano}/Au Electrode	0.75	3–1000	1	Sausage	[31]
DPV	Thionine-ACNTs/GCE[b]	0.8	3–500	1.12	Sausage	[32]
Amperometric	Au/ZnO/MWCNT/GCE	–	0.78–400	0.4	Sausage	[33]
Amperometric	PAA[c]/CNTs/ GCE	–	3–4500	1.0	–	[34]
Amperometric	PANI[d]/MWNTs/Au electrode	–	5–15,000	1.0	–	[35]
Amperometric	G4-NH_4[e]/MWNTs/GCE	0.73	5–50,100–1500	2.0	Sausage	[36]
Amperometric	Ni_7S_6/MWCNT/GCE	0.425	1–4200	0.3	pickle water	[37]
Amperometric	AuNP/rGO HMS[f]/GCE	0.82	5–2600	0.5	tap water	[38]
Amperometric	CDs-Au-N/GCE[g]	0.9	0.1–2000	0.06	lake water	[39]
Amperometric	np-PdFe[h]/GCE	1.2	500–25,500	0.8	sausage	[40]
SWV	MWCNT-Chit/CdTe QD-CTAB/GCE	0.78	1–600	0.30	Pickled vegetable	This work

[a] poly(2-aminothiophenol)

[b] Thionine modified aligned carbon nanotubes electrode

[c] poly(azure A)

[d] polyaniline

[e] Amine-terminated poly(amidoamine) (generation 4.0)

[f] Reduced graphene oxide hollow microspheres

[g] Carbon dots/Au nanohybrids/nafion/GCE

[h] Nanoporous palladium-iron alloy

which does not give an electrochemical signal. Thus, formaldehyde might be added to get rid of the interferences when the electrode was applied to the analysis of commercial samples. Other electro-active small molecular compounds such as ascorbic acid responded at a relatively lower potential (less than 0.4 V) at this electrode, the response potential of nitrite at this electrode was 0.78 V, thus ascorbic acid has no interferences.

Analytical application

Five pickled samples were randomly collected from the local markets and analyzed using the method soon after purchase, at the same time, compared with a UV-Vis method using the splitting samples. It was found that nitrite was detected in almost all the samples with the concentration range of 5.25–22.91 mg Kg^{-1}. Compared with UV-Vis method, the relative error were in the range of −3.21% - 3.19%, showing no remarkably difference ($p > 0.05$) between the SWV method and reference method as illustrated in Table 2.

Conclusions

In this work, a highly selective, reproducible and sensitive enough electrochemical sensor for nitrite determination was fabricated based on CdTe QD-CTAB/Chit-MWCNT composite modified glassy carbon electrode via electrostatic self-assembly strategy. The oxidation peak current of nitrite was significantly increased at a relative low over-potential due to the good conductivity and high surface area. The electrode is easy to operate but substantial skills are needed to construct it. It should be useful in general to prepare sensors based on other quantum dots. Moreover, it was successfully used for

Table 2 Comparison of the SWV method with reference method (UV-Vis) in determination of nitrite in pickled vegetable samples

Samples	SWV method (mg kg^{-1})	UV-Vis method (mg kg^{-1})	Relative error (%)	RSD of the SWV method (%) ($n = 3$)
Sample 1	14.81 ± (0.64)	14.38	3.00	4.34
Sample 2	12.78 ± (0.34)	12.49	−0.86	2.80
Sample 3	17.72 ± (0.68)	17.21	2.97	3.84
Sample 4	5.25 ± (0.21)	5.09	3.19	3.19
Sample 5	22.91 ± (0.11)	23.67	−3.21	1.04

electrochemical detection of nitrite in commercial pickled vegetable foods, it might be applicable for nitrite sensing in other nitrite-containing matrixes.

Acknowledgements Financial support from National Natural Science Foundation of China (31772085), Zhejiang Provincial Natural Science Foundation of China (LY17C200002) and Zhejiang Provincial Collaborative Innovation Centre of Food Safety and Nutrition (2017SICR113) are greatly acknowledged.

Compliance with ethical standards We declares that the three foundations mentioned in article have no competing interests.

References

1. Bryan NS, Alexander DD, Coughlin JR, Milkowski AL, Boffetta P (2012) Ingested nitrate and nitrite and stomach cancer risk: an updated review. Food Chem Toxicol 50(10):3646–3665. https://doi.org/10.1016/j.fct.2012.07.062
2. Cockburn A, Brambilla G, Fernández ML, Arcella D, Bordajandi LR, Cottrill B, van Peteghem C, Dorne JL (2013) Nitrite in feed: from animal health to human health. Toxicol Appl Pharmacol 270(3):209–217. https://doi.org/10.1016/j.taap.2010.11.008
3. Yao W, Byrne RH, Waterbury RD (1998) Determination of Nanomolar concentrations of nitrite and nitrate in natural waters using long path length absorbance spectroscopy. Environ Sci Technol 32(17):2646–2649. https://doi.org/10.1021/es9709583
4. Shah I, Petroczi A, James RA, Naughton DP (2014) Determination of nitrate and nitrite content of dietary supplements using ion chromatography. J Anal Bioanal Tech S12:1–7. https://doi.org/10.4172/2155-9872.S12-003
5. Rotariu L, Lagarde F, Jaffrezic-Renault N, Bala C (2016) Electrochemical biosensors for fast detection of food contaminants – trends and perspective. TrAC Trends Anal Chem 79:80–87. https://doi.org/10.1016/j.trac.2015.12.017
6. Wang QH, Yu LJ, Liu Y, Lin L, Lu RG, Zhu JP, He L, Lu ZL (2017) Methods for the detection and determination of nitrite and nitrate: a review. Talanta 165:709–720. https://doi.org/10.1016/j.talanta.2016.12.044
7. Liu TS, Kang TF, Lu LP, Zhang Y, Cheng SY (2009) Au–Fe(III) nanoparticle modified glassy carbon electrode for electrochemical nitrite sensor. J Electroanal Chem 632(1):197–200. https://doi.org/10.1016/j.jelechem.2009.04.023
8. Zhang D, Fang Y, Miao Z, Ma M, Du X, Takahashi S, J-i A, Chen Q (2013) Direct electrodeposion of reduced graphene oxide and dendritic copper nanoclusters on glassy carbon electrode for electrochemical detection of nitrite. Electrochim Acta 107:656–663. https://doi.org/10.1016/j.electacta.2013.06.015
9. Zhang Y, Yin J, Wang K, Chen P, Ji L (2013) Electrocatalysis and detection of nitrite on a polyaniline-Cu nanocomposite-modified glassy carbon electrode. J Appl Polym Sci 128(5):2971–2976. https://doi.org/10.1002/app.38466
10. Radhakrishnan S, Krishnamoorthy K, Sekar C, Wilson J, Kim SJ (2014) A highly sensitive electrochemical sensor for nitrite detection based on Fe_2O_3 nanoparticles decorated reduced graphene oxide nanosheets. Appl Catal B Environ 148:22–28. https://doi.org/10.1016/j.apcatb.2013.10.044
11. Haldorai Y, Kim JY, Vilian ATE, Heo NS, Huh YS, Han YK (2016) An enzyme-free electrochemical sensor based on reduced graphene oxide/Co_3O_4 nanospindle composite for sensitive detection of nitrite. Sensors Actuators B Chem 227:92–99. https://doi.org/10.1016/j.snb.2015.12.032
12. Zhang ML, Huang DK, Cao Z, Liu YQ, He JL, Xiong JF, Feng ZM, Yin YL (2015) Determination of trace nitrite in pickled food with a nano-composite electrode by electrodepositing ZnO and Pt nanoparticles on MWCNTs substrate. LWT-Food Sci Techonl 64(2):663–670. https://doi.org/10.1016/j.lwt.2015.06.025
13. Yildiz G, Oztekin N, Orbay A, Senkal F (2014) Voltammetric determination of nitrite in meat products using polyvinylimidazole modified carbon paste electrode. Food Chem 152:245–250. https://doi.org/10.1016/j.foodchem.2013.11.123
14. Yin X, Chen Q, Song H, Yang M, Wang H (2013) Sensitive and selective electrochemiluminescent detection of nitrite using dual-stabilizer-capped CdTe quantum dots. Electrochem Commun 34:81–85. https://doi.org/10.1016/j.elecom.2013.04.029
15. Liu X, Guo L, Cheng L, Ju H (2009) Determination of nitrite based on its quenching effect on anodic electrochemiluminescence of CdSe quantum dots. Talanta 78(3):691–694. https://doi.org/10.1016/j.talanta.2008.12.035
16. Zhang Z, Duan F, He L, Peng D, Yan F, Wang M, Zong W, Jia C (2016) Electrochemical clenbuterol immunosensor based on a gold electrode modified with zinc sulfide quantum dots and polyaniline. Microchim Acta 183(3):1089–1097. https://doi.org/10.1007/s00604-015-1730-2
17. Khene S, Moeno S, Nyokong T (2011) Voltammetry and electrochemical impedance spectroscopy of gold electrodes modified with CdTe quantum dots and their conjugates with nickel tetraamino phthalocyanine. Polyhedron 30(12):2162–2170. https://doi.org/10.1016/j.poly.2011.06.002
18. Yang R, Miao D, Liang Y, Qu L, Li J, PdB H (2015) Ultrasensitive electrochemical sensor based on CdTe quantum dots-decorated poly(diallyldimethylammonium chloride)-functionalized graphene nanocomposite modified glassy carbon electrode for the determination of puerarin in biological samples. Electrochim Acta 173:839–846. https://doi.org/10.1016/j.electacta.2015.05.139
19. Li J, Li X, Yang R, Qu L, Harrington PB (2013) A sensitive electrochemical chlorophenols sensor based on nanocomposite of ZnSe quantum dots and cetyltrimethylammonium bromide. Anal Chim Acta 804:76–83. https://doi.org/10.1016/j.aca.2013.09.049
20. Trigueiro JPC, Silva GG, Pereira FV, Lavall RL (2014) Layer-by-layer assembled films of multi-walled carbon nanotubes with chitosan and cellulose nanocrystals. J Colloid Interface Sci 432:214–220. https://doi.org/10.1016/j.jcis.2014.07.001
21. Zarate Triviño DG, Prokhorov E, Luna Bárcenas G, Mendez Nonell J, González Campos JB, Elizalde Peña E, Mota Morales JD, Santiago Jacinto P, Terrones M, Gómez Salazar S, Nuño Donlucas SM, Sanchez IC (2015) The effect of CNT functionalization on electrical and relaxation phenomena in MWCNT/chitosan composites. Mater Chem Phys 155:252–261. https://doi.org/10.1016/j.matchemphys.2015.02.041
22. Ran G, Chen C, Gu C (2015) Serotonin sensor based on a glassy carbon electrode modified with multiwalled carbon nanotubes, chitosan and poly(p-aminobenzenesulfonate). Microchim Acta 182(7):1323–1328. https://doi.org/10.1007/s00604-015-1454-3
23. Zhou G, Lu Y, Zhang H, Chen Y, Yu Y, Gao J, Sun D, Zhang G, Zou H, Zhong Y (2013) A novel pulsed drug-delivery system: polyelectrolyte layer-by-layer coating of chitosan–alginate microgels. Int J Nanomedicine 8:877–887. https://doi.org/10.2147/IJN.S38144
24. Dong S, Guan W, Lu C (2013) Quantum dots in organo-modified layered double hydroxide framework-improved peroxynitrous acid chemiluminescence for nitrite sensing. Sensors Actuators B Chem 188:597–602. https://doi.org/10.1016/j.snb.2013.07.060
25. Unnikrishnan B, Mani V, Chen S-M (2012) Highly sensitive amperometric sensor for carbamazepine determination based on electrochemically reduced graphene oxide–single-walled carbon nanotube composite film. Sensors Actuators B Chem 173:274–280. https://doi.org/10.1016/j.snb.2012.06.088

26. Liu Q, Lu X, Li J, Yao X, Li J (2007) Direct electrochemistry of glucose oxidase and electrochemical biosensing of glucose on quantum dots/carbon nanotubes electrodes. Biosens Bioelectron 22(12):3203–3209. https://doi.org/10.1016/j.bios.2007.02.013
27. Kamyabi MA, Aghajanloo F (2008) Electrocatalytic oxidation and determination of nitrite on carbon paste electrode modified with oxovanadium(IV)-4-methyl salophen. J Electroanal Chem 614(1): 157–165. https://doi.org/10.1016/j.jelechem.2007.11.026
28. Canevari TC, Luz RCS, Gushikem Y (2008) Electrocatalytic determination of nitrite on a rigid disk electrode having cobalt Phthalocyanine prepared in situ. Electroanalysis 20(7):765–770. https://doi.org/10.1002/elan.200704082
29. Doherty AP, Stanley MA, Leech D, Vos JG (1996) Oxidative detection of nitrite at an electrocatalytic [Ru(bipy)2poly-(4-vinylpyridine)10Cl]cl electrochemical sensor applied for the flow injection determination of nitrate using a Cu/Cd reductor column. Anal Chim Acta 319(1):111–120. https://doi.org/10.1016/0003-2670(95)00475-0
30. Guidelli R, Pergola F, Raspi G (1972) Voltammetric behavior of nitrite ion on platinum in neutral and weakly acidic media. Anal Chem 44(4):745–755. https://doi.org/10.1021/ac60312a018
31. Saber-Tehrani M, Pourhabib A, Husain SW, Arvand M (2013) A simple and efficient electrochemical sensor for nitrite determination in food samples based on Pt nanoparticles distributed poly(2-aminothiophenol) modified electrode. Food Anal Methods 6(5): 1300–1307. https://doi.org/10.1007/s12161-012-9543-y
32. Zhao K, Song H, Zhuang S, Dai L, He P, Fang Y (2007) Determination of nitrite with the electrocatalytic property to the oxidation of nitrite on thionine modified aligned carbon nanotubes. Electrochem Commun 9(1):65–70. https://doi.org/10.1016/j.elecom.2006.07.001
33. Lin AJ, Wen Y, Zhang LJ, Lu B, Li Y, Jiao YZ, Yang HF (2011) Layer-by-layer construction of multi-walled carbon nanotubes, zinc oxide, and gold nanoparticles integrated composite electrode for nitrite detection. Electrochim Acta 56(3):1030–1036. https://doi.org/10.1016/j.electacta.2010.10.058
34. Zeng J, Wei W, Zhai X, Yang P, Yin J, Wu L, Liu X, Liu K, Gong S (2006) Assemble-electrodeposited ultrathin conducting poly(azure A) at a carbon nanotube-modified glassy carbon electrode, and its electrocatalytic properties to the reduction of nitrite. Microchim Acta 155(3):379–386. https://doi.org/10.1007/s00604-006-0570-5
35. Guo M, Chen J, Li J, Tao B, Yao S (2005) Fabrication of polyaniline/carbon nanotube composite modified electrode and its electrocatalytic property to the reduction of nitrite. Anal Chim Acta 532(1):71–77. https://doi.org/10.1016/j.aca.2004.10.045
36. Zhu N, Xu Q, Li S, Gao H (2009) Electrochemical determination of nitrite based on poly(amidoamine) dendrimer-modified carbon nanotubes for nitrite oxidation. Electrochem Commun 11(12): 2308–2311. https://doi.org/10.1016/j.elecom.2009.10.018
37. Wu W, Li Y, Jin J, Wu H, Wang S, Ding Y, Ou J (2016) Sensing nitrite with a glassy carbon electrode modified with a three-dimensional network consisting of Ni7S6 and multi-walled carbon nanotubes. Microchim Acta 183(12):3159–3166. https://doi.org/10.1007/s00604-016-1961-x
38. Zhang F, Yuan Y, Zheng Y, Wang H, Liu T, Hou S (2017) A glassy carbon electrode modified with gold nanoparticle-encapsulated graphene oxide hollow microspheres for voltammetric sensing of nitrite. Microchim Acta 184(6):1565–1572. https://doi.org/10.1007/s00604-017-2264-6
39. Zhuang Z, Lin H, Zhang X, Qiu F, Yang H (2016) A glassy carbon electrode modified with carbon dots and gold nanoparticles for enhanced electrocatalytic oxidation and detection of nitrite. Microchim Acta 183(10):2807–2814. https://doi.org/10.1007/s00604-016-1931-3
40. Wang J, Zhou H, Fan D, Zhao D, Xu C (2015) A glassy carbon electrode modified with nanoporous PdFe alloy for highly sensitive continuous determination of nitrite. Microchim Acta 182(5):1055–1061. https://doi.org/10.1007/s00604-014-1432-1